Journal of Power Sources 218 (2012) 244–249

Contents lists available at SciVerse ScienceDirect

Journal of Power Sources

journal homepage: www.elsevier.com/locate/jpowsour

Electrolysis of H_2O and CO_2 in an oxygen-ion conducting solid oxide electrolyzer with a $La_{0.2}Sr_{0.8}TiO_{3+\delta}$ composite cathode

Shisong Li [a], Yuanxin Li [a], Yun Gan [a], Kui Xie [a,*], Guangyao Meng [a,b]

[a] Department of Energy Materials, School of Materials Science and Engineering, Hefei University of Technology, No. 193 Tunxi Road, Hefei, Anhui 230026, China
[b] Department of Materials Science and Engineering, University of Science and Technology of China, No. 96 Jinzhai Road, Hefei, Anhui 230026, China

HIGHLIGHTS

- $La_{0.2}Sr_{0.8}TiO_{3+\delta}$ is a promising cathode of SOE at intermediate temperature.
- The electrolysis of H_2O and CO_2 cathode is efficient in SOE with a $La_{0.2}Sr_{0.8}TiO_{3+\delta}$.
- The main process is reduction of $La_{0.2}Sr_{0.8}TiO_{3+\delta}$ at low voltages.

ARTICLE INFO

Article history:
Received 30 April 2012
Received in revised form
10 June 2012
Accepted 11 June 2012
Available online 7 July 2012

Keywords:
Solid oxide electrolysis cells
Cathode
Steam electrolysis
Carbon dioxide electrolysis
$La_{0.2}Sr_{0.8}TiO_{3\pm\delta}$

ABSTRACT

Solid oxide electrolyzers have attracted a great deal of interest in recent years because they can convert electrical energy into chemical energy with high efficiency. Ni/YSZ cathodes are generally utilized for high temperature electrolysis of H_2O and CO_2 in oxygen-ion conducting solid oxide electrolyzers; however, such electrodes can only operate under reducing conditions. In an atmosphere without a flow of reducing gas, cathodes based on $La_{0.2}Sr_{0.8}TiO_{3+\delta}$ (LST) are a promising alternative. Solid Oxide Electrolyzers with LST cathodes without pre-reduction were used at 700 °C for the electrolysis of 3%H_2O/97% N_2 and 100%CO_2, and promising polarization impedance data were obtained in both atmospheres. The electrochemical results indicated that the electrochemical reduction of the $La_{0.2}Sr_{0.8}TiO_{3+\delta}$ cathode was the main process at low electrical voltages, while the electrolysis was the main process at high voltages because ion transportation in the electrolyte limited the overall efficiency. The electrolysis of H_2O was determined to be more efficient than the electrolysis of CO_2 under the same conditions. The Faraday efficiencies of H_2O and CO_2 were 85.0% and 24.7%, respectively, at 700 °C and a 2 V applied potential.

1. Introduction

Solid oxide electrolyzers have attracted a great deal of interest in recent years because they can convert electrical energy into chemical energy with high efficiency [1–3]. Solid oxide electrolyzers can exploit available heat streams to maximize the electrical efficiency and can operate at high temperature which offers both thermodynamic and kinetic advantages for electrolysis. Using external electricity, oxygen-ion conducting solid oxide electrolyzers are able to electrolyze steam into hydrogen as well as oxygen and carbon dioxide into carbon monoxide and oxygen [1,2]. At the cathode, CO_2 and H_2O molecules are electrochemically reduced into CO and H_2, respectively, under an external applied potential. The O^{2-} ions are transported through the oxygen-ion conducting electrolyte membrane to the anode compartment where O_2 gas is formed and released. Since the 1990s, many investigations have focused on the development of efficient solid oxide electrolyzers for high temperature H_2O electrolysis. Only a limited number of studies reported the electrolysis of CO_2 in the gas phase; however, the studies mainly used palladium, platinum and nickel for the fuel electrode [4]. In addition, coelectrolysis of H_2O/CO_2 has also been investigated to synthesize H_2/CO, which can be further converted into hydrocarbons in a Fischer–Tropsch-type synthesis using either an appropriate metal catalyst or other methods [5,6]. Therefore, using solid oxide electrolyzers for recycling or reuse of CO_2 from energy systems (or CO_2 capture from air) would be an attractive alternative to storage of CO_2 and would provide CO_2-neutral synthetic hydrocarbon fuels, which lead to the world toward the use of renewable energy.

Currently, most reports of high temperature steam electrolysis and carbon dioxide electrolysis have been preferentially performed with Ni/YSZ composite cathode in oxygen ion conducting solid oxide electrolyzers. However, a significant concentration of H_2 or

* Corresponding author. Tel.: +86 551 2905413.
E-mail address: xiekui@hfut.edu.cn (K. Xie).

0378-7753/$ – see front matter © 2012 Elsevier B.V. All rights reserved.
http://dx.doi.org/10.1016/j.jpowsour.2012.06.046

CO flowing over Ni cermet, typically with pre-reduction of the cathode, is required to avoid oxidation to NiO [4,5,7]. Oxidation would cause a loss of electronic conductivity and potentially lead to mechanical failure of the electrode [8,9]. The perovskite, $(La_{0.75}Sr_{0.25})_{0.95}Mn_{0.5}Cr_{0.5}O_3$ (LSCM), is an active and redox-stable material that has attracted attention as a high temperature solid oxide fuel cell anode [10–13]. Irvine et al. have recently demonstrated the efficient electrolysis of H_2O and CO_2 based on an LSCM cathode without using a flow of reducing gases. However, the p-type conduction mechanism of the LSCM was not ideally adapted to the strong reducing potential that leads to a large electrode polarization resistance [14]. In addition, strong reducing potentials can also result in chemical and structural changes in the LSCM cathodes. To further optimize electrolysis and achieve a higher efficiency, a ceramic cathode (i.e., fuel electrode) that has a n-type conduction mechanism upon reduction and an excellent electrocatalytic activity is desirable. Therefore, a ceramic cathode would be a good fit for the strongly reducing conditions that occur in the cathode and would result in better electrode polarization performances. The perovskite, $La_xSr_{1-x}TiO_{3+\delta}$ (LST), is an active, redox-stable material that has high n-type conductivity upon reduction, which has led to the material receiving a great deal of attention in the field of high temperature solid oxide fuel cell anodes [15–17]. Ceramic $La_xSr_{1-x}TiO_{3\pm\delta}$ is a p-type conductor before reduction with a thermal coefficient of approximately 5×10^{-6} K^{-1}, which is a smaller value than the value for YSZ. The introduction of La into Sr site promotes the reduction of LST under reducing conditions. The LST is a typical n-type conductor upon reduction with a conductivity as high as 30 S cm^{-1} at intermediate temperature in wet H_2. Ceramic LST is stable and the perovskite structure is retained upon treatment in pure H_2 at 1400 °C. These properties are highly important for the applications in the field of ceramic fuel electrodes.

In this work, a $La_{0.2}Sr_{0.8}TiO_{3+\delta}/Ce_{0.8}Gd_{0.2}O_{2-\delta}$-composite cathode was investigated for use in the direct electrolysis of H_2O and CO_2 based on an oxygen-ion conducting solid oxide electrolyzer, in which no pre-reduction of the cathode was performed and no reducing gas was introduced. The cathode performance and the electrochemical processes of the electrolyses of different gases were investigated and evaluated. The differences between the direct electrolyses of H_2O and CO_2 were also studied.

2. Experimental

A 2-mm-thick 8YSZ disc electrolyte support was prepared by dry-pressing [18] the 8YSZ powder (Pi-Chem powder) into a green disk with a diameter of ~30 mm, and then the disk was sintered in air at 1350 °C for 10 h. The two surfaces of the obtained YSZ electrolyte support were mechanically polished with sand paper (1000 mesh), and then was ultrasonically cleaned several times while immersed in ethanol and distilled water. Finally, the disks were dried in air overnight. Ceramic $La_{0.2}Sr_{0.8}TiO_{3+\delta}$ (LST) powders were synthesized by a conventional solid-state reaction method described elsewhere [16]. Briefly, appropriate amounts of La_2O_3, $SrCO_3$ and TiO_2 were ball-milled in acetone, and then dried in air to obtain whitish-yellow powders. The resultant powders were axially pelletized at 200 MPa and then fired in air at 1300 °C for 10 h. Subsequently, powder X-ray diffraction ($\Theta \sim 0.50°$ min^{-1}) was performed to analyze the phase purity of the LST powders. The cathode slurry was prepared by directly milling a commercially obtained fine $Ce_{0.9}Gd_{0.1}O_{2-\delta}$ (CGO) (Pi-Chem powder) powder with the LST powder at a 50:50 weight ratio in a mortar. In addition, cellulose was added to create porosity in the cathode. Similarly, the anode was prepared from a slurry that consisted of $(La_{0.8}Sr_{0.2})_{0.95}MnO_{3-\delta}$ (LSM) (Pi-Chem powder) and CGO powders at a 50:50 weight ratio in alpha-terpineol with the cellulose additive. The cathode and anode were screen-printed onto the electrolyte in symmetric positions with areas of 1 cm^2, and then the sample was heat treated at 1050 °C (2 °C min^{-1}) for 3 h in air to assemble a single cell [19]. The current collection layer was made with silver paste (silver conductive ink, Alfa Aesar), which was printed onto both electrode surfaces, and then heat treated at 550 °C (3 °C min^{-1}) for 30 min in air. The external circuit was fabricated with silver electrical wire (0.1 mm in diameter), which was connected to both current collectors using silver paste and then heat treated at 550 °C (3 °C min^{-1}) for 30 min in air. The single solid oxide electrolyzer was sealed to a home-made testing jig using ceramic paste (Aremco, Ceramabond 552) for the electrochemical measurements without any further treatments (e.g., cathode reduction with hydrogen). The LSM-based anode was exposed to static air, whereas H_2O and CO_2 were supplied to the cathode compartment. The CO_2 and H_2O gas flows were controlled via a mass flow meter and a syringe pump, respectively. The experiment was performed at 700 °C under external electrical voltages to achieve the electrochemical reduction. Electrochemical measurements (e.g., AC impedance, current–voltage (I–V) and open circuit voltage (OCV)) were performed using a Schlumberger Solartron 1255 Frequency Response Analyzer coupled with a 1287 Electrochemical Interface controlled by Zplot electrochemical impedance software. The output gas from cathode was connected with a U-type cooling tube in dry ice to eliminate steam contamination in the mixture of gases before supplied to an attached Prolab 300 (Thermoscientific) mass spectrometer (MS). The microstructure of the as-prepared electrolyzer was characterized using a scanning electron microscope (JEOL 5600) after test. The steam electrolysis was performed first, and then the CO_2 electrolysis was performed after the electrolyzer reached equilibrium. After completion of the electrolysis experiments, the OCVs of the electrolyzers were acquired to determine the status of the electrolyzers.

The $La_{0.2}Sr_{0.8}TiO_{3+\delta}$ (LST) cathode was prepared via a solid-state reaction method followed by heat treatment in air at 1200 °C, which resulted in the formation of a white-yellowish powder. As shown in Fig. 1, only strong peaks that corresponded to the perovskite LST were observed in the XRD pattern of the as-prepared sample [17]. The composite cathode $La_{0.2}Sr_{0.8}TiO_{3+\delta}/Ce_{0.8}Gd_{0.2}O_{2-\delta}$ (LST/CGO) and composite anode $(La_{0.8}Sr_{0.2})_{0.95}MnO_{3-\delta}/Ce_{0.8}Gd_{0.2}O_{2-\delta}$ (LSM/

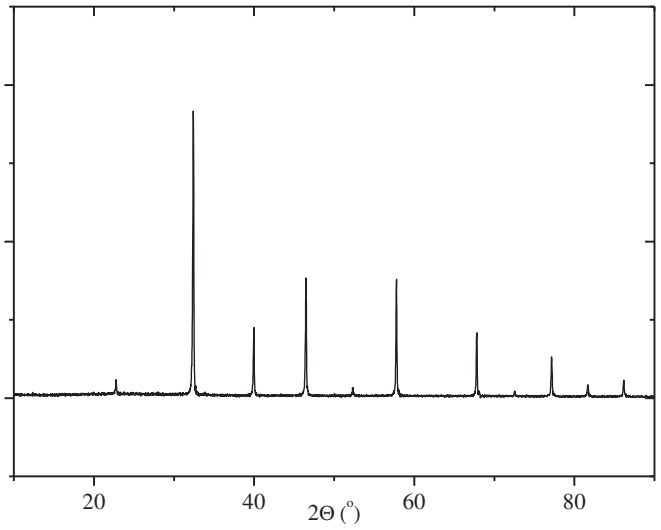

Fig. 1. XRD pattern of the $La_{0.2}Sr_{0.8}TiO_{3+\delta}$ cathode prepared by solid-state reaction method followed by heat treatment at 1200 °C in air.

CGO) were used to construct a single solid oxide electrolyzer based on a 2.0-mm-thick YSZ electrolyte support. The microstructure of the electrolyzer is shown in Fig. 2. The porous 20-μm-thick cathode and anode layers adhered to the electrolyte very well. The porous silver current collector layer was approximately 2 μm in thickness.

3. Results and discussions

Fig. 3 shows the open circuit voltages of solid oxide electrolyzer with various flowing rates of 10%H_2O/N_2 input gas into the cathode, while the anode was exposed in static air. The OCVs were approximately 0.075 V at 1.0 ml min^{-1}, 0.085 V at 2.0 ml min^{-1}, 0.12 V at 10.0 ml min^{-1} and 0.14 V at 20.0 ml min^{-1}. At this point, the electrochemical cell was an oxygen-concentration cell, and the OCV mainly resulted from the differences of oxygen concentration across two electrodes. The oxygen concentration caused by the thermal splitting of steam might be lower at a high steam flow rate than a low flow rate, which is one possible explanation for the different OCVs that resulted from the variation in steam flow rates. Fig. 4 shows the measurement of current density versus applied voltage for steam electrolysis at 700 °C with a flow rate 20 ml min^{-1}. The OCV was approximately 0.14 V, which was caused by the oxygen concentration gradient across both electrodes. Additionally, the current–voltage (I–V) curve was non-linear: a clear change in slope was observed at approximately 1.4 V, which was the anticipated onset of H_2 production from the steam electrolysis. The calculated cell resistance from the I–V curve above 1.4 V was approximately 10 Ω cm^2, whereas the cell resistance was much larger and reached ∼100 Ω cm^2 at low voltages. The expected ionic resistance of such a YSZ pellet was approximately 6 Ω cm^2 at 700 °C [20], which indicates that the ionic resistance of the YSZ electrolyte largely contributed to the total cell resistance at higher potentials, while the electrode polarization resistance dominated the total cell resistance at low voltages. The final current density of the solid oxide electrolyzer reached ∼90 mA cm^{-2} with an applied voltage of 2 V at 700 °C.

To further investigate the electrochemical process of the electrolyzer at a variety of external potentials, in situ AC impedance spectroscopy was performed at applied dc voltages that ranged from 0 to 2 V versus OCV shown in Figs. 5 and 6 The impedance curve was modeled with the Zplot electrochemical impedance software to determine the first and second intercepts with real parts. The first intercept represents the series resistance of the cell (R_s), and the difference between the two intercepts was used as the electrode polarization resistance (R_p). As can be observed in Fig. 5,

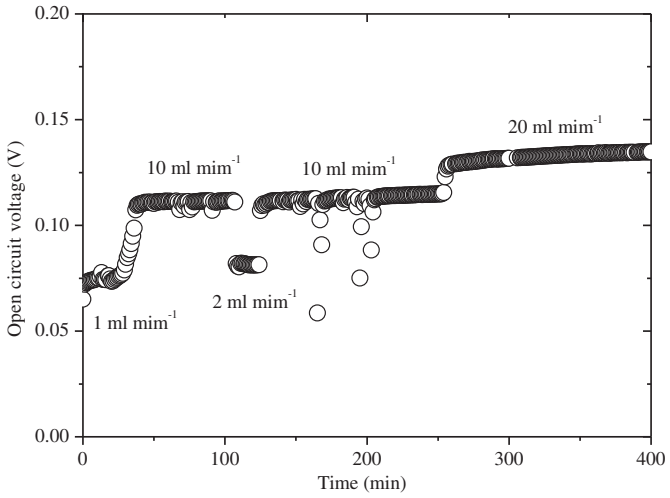

Fig. 3. Open circuit voltage of the solid oxide electrolyzer versus various flow rates of steam at the cathode at 700 °C.

the R_s only changed by a small amount, while the R_p drastically decreased versus applied electrical voltages. The slight variation of R_s might have been related to changes in the R_p affecting the intercept and, particularly for lower R_p values, enhancement of the lateral conductivity in the cathode at high potentials [6]. As shown in Fig. 5, the R_p significantly decreased from ∼100 Ω cm^2 for open circuit to ∼12 Ω cm^2 at 1.2 V, which indicates that the electrode performance improved under higher external potentials.

However, the R_p continued to decrease versus the applied external potentials, whereas the R_p decreased to ∼1.2 Ω cm^2 at 2.0 V. The anode LSM is a mixed conductor with very good p-type conduction at intermediate temperatures. Therefore, the applied voltage would lead to an oxidizing atmosphere at the anode, which would further improve the LSM anode performance. On the contrary, the LST cathode is not pre-reduced and generally shows ∼0.001 S cm^{-1} at 700 °C in air, which would dominate the electrode polarization resistance in such a solid oxide electrolyzer [15]. However, the LST ceramic shows excellent conductivity after being strongly reduced (e.g., reduced with hydrogen at 1400 °C for 20 h) [16,17]. In the experiment in this report, the increased voltages would gradually and electrochemically reduce the LST-based cathode ($Ti^{4+} \rightarrow Ti^{3+}$) up to 2 V in situ, which resulted in contentiously improved mixed conductivities and electrocatalytic

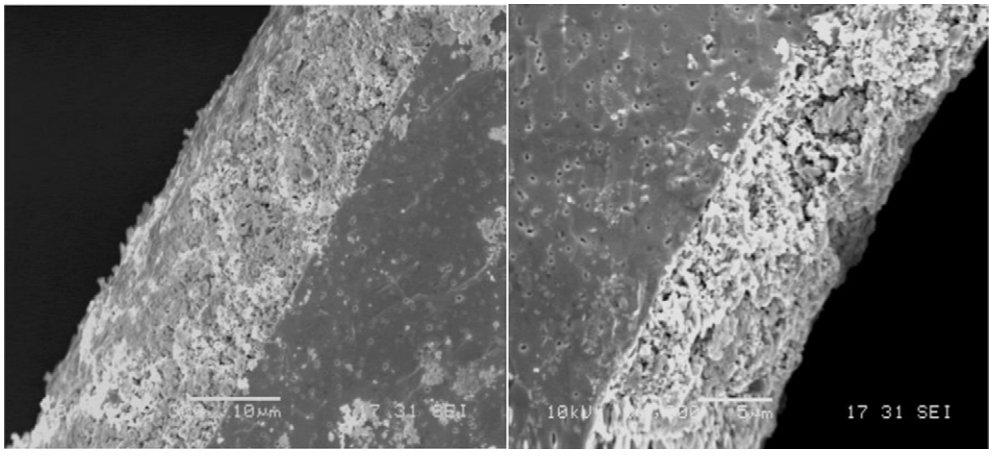

Fig. 2. Microstructure of the solid oxide electrolyzer with a $La_{0.2}Sr_{0.8}TiO_{3+\delta}$/YSZ/$(La_{0.8}Sr_{0.2})_{0.95}MnO_{3-\delta}$ (left to right) configuration.

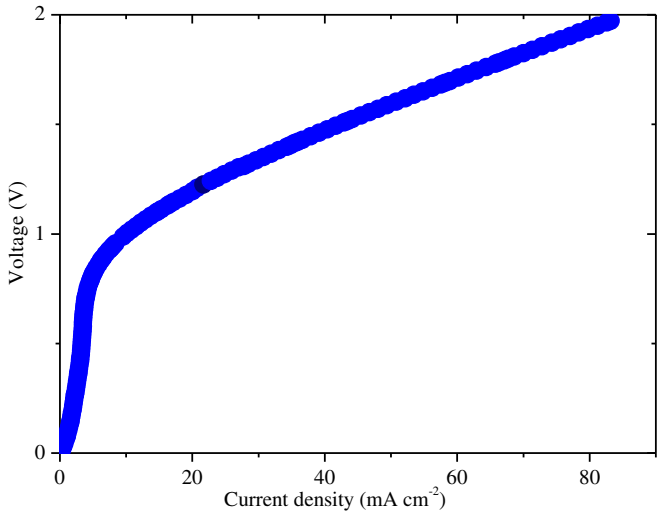

Fig. 4. *I–V* curve of the solid oxide electrolyzer cell for steam electrolysis at 700 °C with the applied voltage versus the OCV.

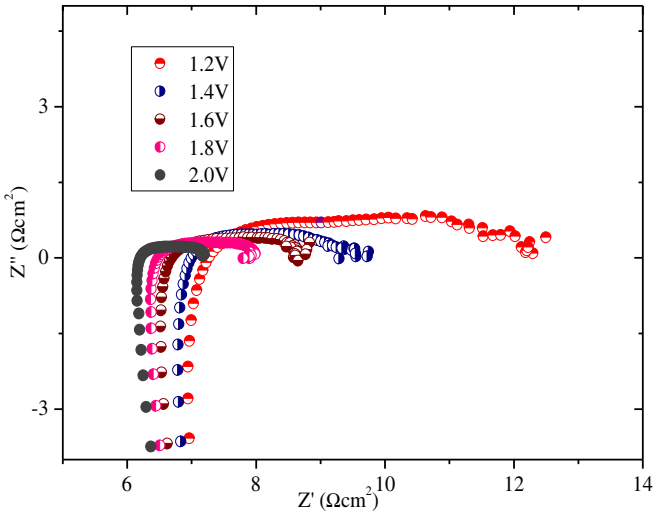

Fig. 6. In situ AC impedance of solid oxide electrolyzer for steam electrolysis at different applied potentials versus OCV at 700 °C.

performances in the electrolyzer [21]. This is a significant advantage of an LST ceramic cathode in contrast to a traditional Ni cermet cathode, which requires a high concentration of reducing gas (e.g., hydrogen) for pre-reduction. Therefore, reduced LST materials with n-type conduction well-suit the strongly reducing conditions of the electrolyzer cathode, whereas other ceramic materials (e.g., LSCM) might undergo adverse chemical changes, while remaining functional without a flow of hydrogen [1].

There are two main processes that occurred with an applied external voltage that ranged from 0 to 2 V in the solid oxide electrolyzer at 700 °C. The significant change of the R_p at potentials below ~1.2 V indicates that the electrochemical reduction of the LST cathode should be the dominant process. However, above ~1.2 V, the dominate process shifted from the electrochemical reduction of the LST electrode to steam electrolysis. Although the R_p at higher voltages continuously improved, only a small change of R_p was observed, which indicates that the high-voltage process might be accompanied by the electrochemical reduction of LST-based cathode and the oxidation of LSM anode. However, the high electrical voltages would cause the R_p to decrease further because the kinetics and thermodynamics for the electrode reactions were favorable. In contrast, steam electrolysis dominated the electrochemical process at high voltages. The AC impedance spectroscopy was generally consistent with the values obtained from the gradients of the *I–V* curves. It is reasonable to believe that the oxygen-ion transport in the YSZ electrolyte is the rate limiting step for steam electrolysis at high electrical voltages because the R_p only corresponds to ~25% of the R_s under the same conditions.

Fig. 7 shows the short-term performance of steam electrolysis at 700 °C, where the current density reaches ~90 mA cm^{-2} with an applied electrical voltage of 2 V. The current density was generally stable, which indicates the steady electrochemical process used steam to simultaneously produce hydrogen at the cathode and oxygen at the anode. However, the steady electrolysis process also shows the excellent stability of the electrode materials under extreme conditions (i.e., the strongly reducing and oxidizing conditions at the cathode and anode, respectively). Only the short-time performance of H_2O electrolysis at 700 °C is reported; however, a long-time test (~20 h) was performed to further confirm the stability of the LST electrode. As shown in Fig. 8, the

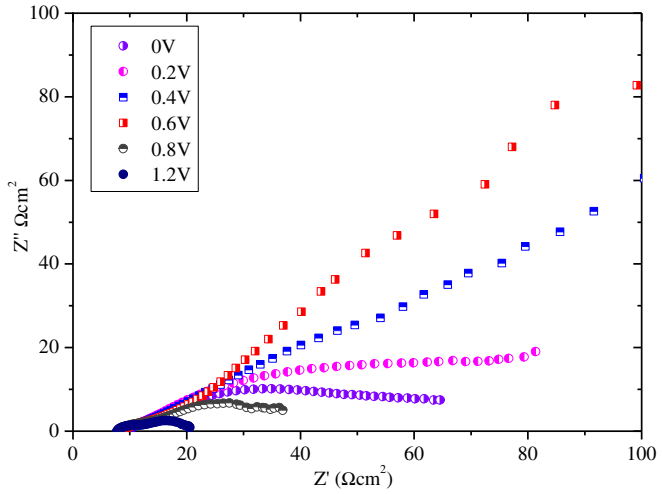

Fig. 5. In situ AC impedance of the solid oxide electrolyzer cell for steam electrolysis at different applied potentials versus OCV at 700 °C.

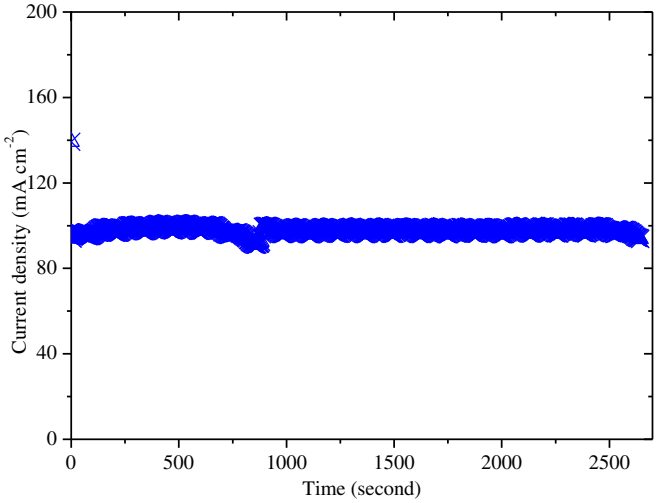

Fig. 7. Short-term performance of the solid oxide electrolyzer for H_2O electrolysis at 2 V versus OCV at 700 °C.

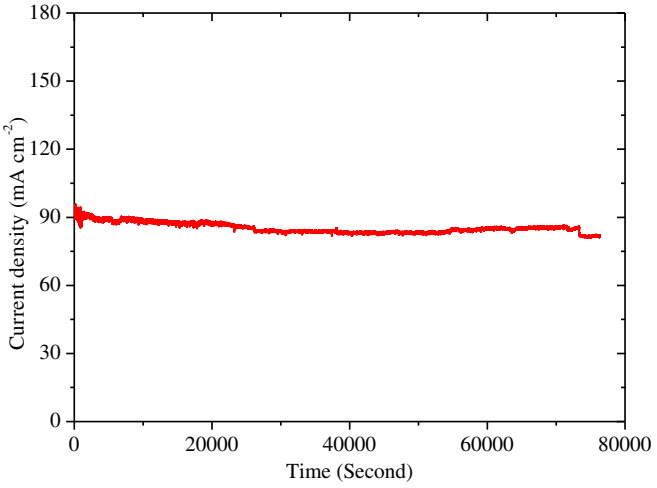

Fig. 8. Long-term performance of solid oxide electrolyzer for H_2O electrolysis at 2 V versus OCV and 700 °C.

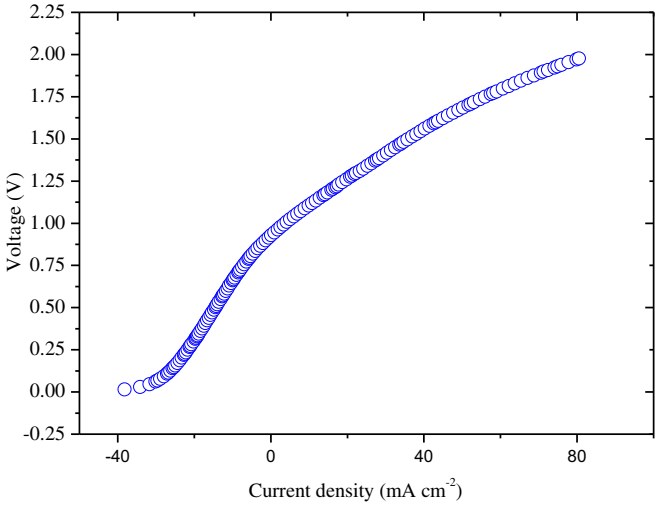

Fig. 10. *I–V* curve of the solid oxide electrolyzer for CO_2 electrolysis at 700 °C where the voltage is applied versus the reference.

current was stable in the long-term test, which further demonstrates that the LST electrode was highly stable because any decomposition of the LST electrode would lead to a decreased performance in electrolysis. As shown in Fig. 9, hydrogen was produced at a rate of ~1.92 ml min^{-1} with a Faradaic yield of 85.0%. Upon completion of the electrolysis process, the OCV was 1.05 V. At this point, the electrolyzer was considered to be in a fuel cell mode.

After completion of the team electrolysis, the solid oxide electrolyzer was held under open circuit conditions with CO_2 flowing over the cathode until the cell voltage reached equilibrium (~1 h was required) to eliminate the residual hydrogen. Before the CO_2 electrolysis experiments began, the OCV was ~0.9 V, which was greater than the OCVs (0.16–0.60 V) for a CO_2/air concentration cell [22]. This high OCV value might be attributed to residual hydrogen in the cathode, which would lead to higher OCV in fuel cell mode. However, the redox process of the LST might be reversible which would lead to the absence of conductivity in the LST cathode. At this stage, the OCV with CO_2 might have been an artifact because the LST cathode was insufficiently conductive in pure CO_2 before electrical voltages for reduction were applied [6]. Fig. 10 shows the current density versus applied voltages for CO_2 electrolysis at 700 °C, which the flow rate was 20 ml min^{-1}. The OCV is ~1.1 V for a solid oxide fuel cell that directly uses CO [23]. Therefore, the CO_2 electrolysis was expected to begin at similar voltage versus the reference. The negative current reached ~−40 mA cm^{-2} under open-circuit conditions and continuously decreased as the applied external voltage decreased below ~1.2 V. At this stage, the current might be related to the transportation of oxygen, (i.e., the electrochemical permeation of oxygen), from anode to cathode. A similar *I–V* curve with a slop change that occurred at approximately 1.2 V was observed for CO_2 electrolysis, which the onset of CO production was anticipated at approximately 1.2 V. However, the change in slope was smaller than the slope change observed for steam electrolysis, which might be attributed to pre-reduction of LST to some extent during the steam electrolysis.

As discussed for steam electrolysis, the electrochemical process for CO_2 electrolysis should be fairly similar. As shown in Figs. 10 and 11, the electrochemical reduction of the LST cathode was the main process at low voltages, which the electrode polarization dominated the cell performances. However, electrolysis of CO_2 was the

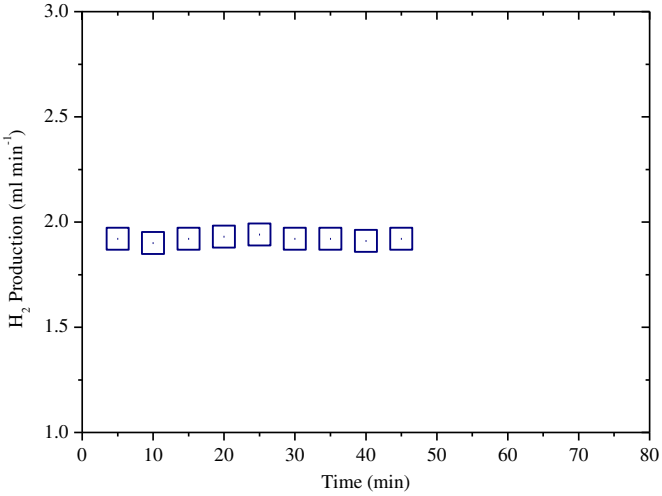

Fig. 9. H_2 production of the solid oxide electrolyzer from steam electrolysis at 2 V versus OCV at 700 °C.

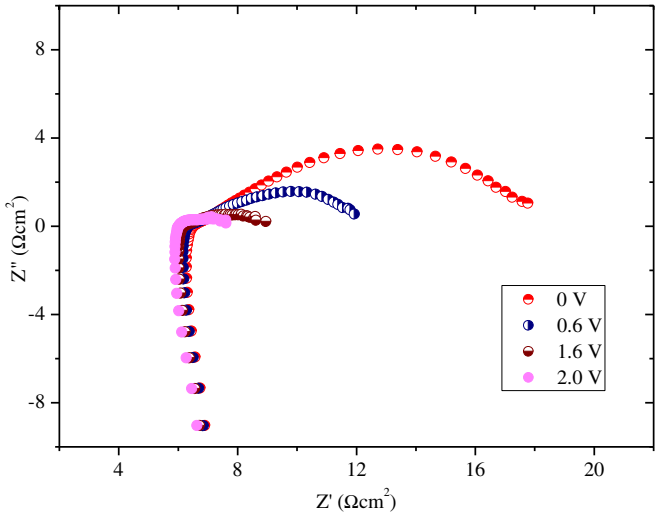

Fig. 11. In situ AC impedance of the solid oxide electrolyzer for CO_2 electrolysis at different applied potentials and 700 °C.

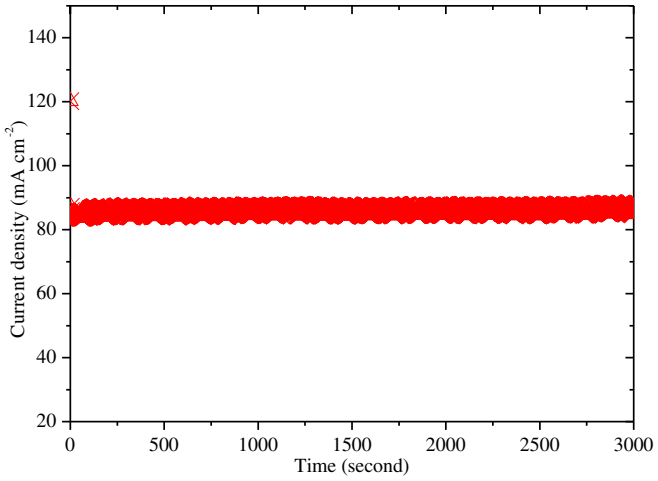

Fig. 12. Short-term performance of the solid oxide electrolyzer for CO_2 electrolysis at 2 V and 700 °C.

dominant process at high voltages. This process caused the electrochemical reduction of the LST cathode and oxidation of the LSM anode to be enhanced, which led to better electrode polarizations. In contrast to the steam electrolysis data, the electrolysis of CO_2 shows similar AC impedance data under high voltages. Fig. 12 shows the short-term performance of CO_2 electrolysis under 2 V, in which the current density reached ~80 mA cm^{-2} at 700 °C. The stable current density indicated the steady electrochemical reduction of CO_2 at the cathode and efficient production of oxygen at the anode. However, the steady electrolysis process might indicate that no serious carbon deposition occurred on the LST composite cathode because serious coking of the cathode leads to significant degradation of electrolysis performance. To further confirm the absence of carbon deposition, long-term electrolysis tests and element analysis are required, which is the focus of the future work of this project. As shown in Fig. 13, carbon monoxide was produced at a rate of ~0.56 ml min^{-1} with a Faradaic yield of 24.7%, which is much lower than the value obtained for steam electrolysis under similar conditions. Previous experiments have shown that low efficiency might be related to CO_2 starvation at the cathode because the adsorption of CO_2 might limit the overall performance [4]. Therefore, the low current efficiency may be

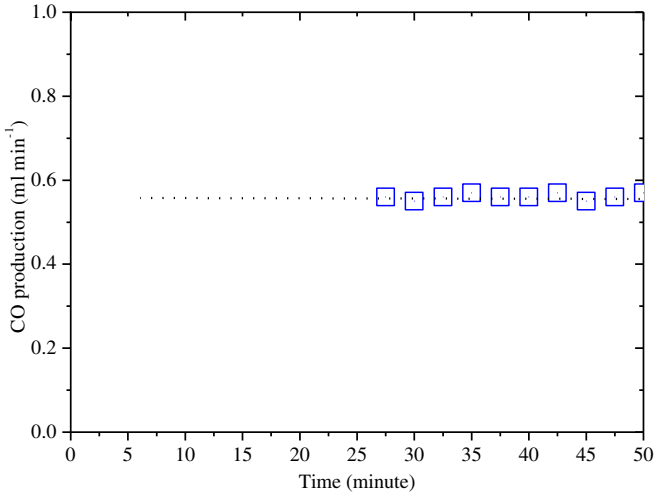

Fig. 13. The production of CO from CO_2 electrolysis in the solid oxide electrolyzer at 2 V applied potential and 700 °C.

Table 1
Comparison of the electrolysis performance of the solid oxide electrolyzer for H_2O and CO_2.

	H_2	CO	Faraday efficiency
H_2O	1.92 ml min^{-1}	–	85.0%
CO_2	–	0.56 ml min^{-1}	24.7%

related to the CO_2 starvation because the CO_2 was adsorbed onto the electrode before electrochemical reduction occurred, which was a limiting step. Normally, H_2 production is detected at the cathode because the detection of oxygen is difficult; however, the isotope method can be used for the detection of oxygen. The electronic conduction in YSZ electrolyte will cause a loss of current efficiency as CO_2 starvation occurs, which is believed to be the reason why current efficiency is relatively low [24]. Upon completion of the CO_2 electrolysis, the OCV reached 1.01 V. At this point, the electrolyzer was in an SOFC mode fueled with CO.

4. Conclusions

In this work, the efficient electrolysis of H_2O and CO_2 was demonstrated in an oxygen-ion conducting solid oxide electrolyzer with a $La_{0.2}Sr_{0.8}TiO_{3+\delta}$ (LST) cathode. In an atmosphere without a flowing reducing gas and without pre-reduction, the LST cathode provides promising electrode polarizations for the direct electrolysis of H_2O and CO_2. The electrochemical results indicated that the reduction of the LST cathode was the main process at low electrical voltages, whereas the electrolysis was the major process at high voltages. This result was attributed to the ionic transportation in electrolyte, which limited the overall efficiency. The Faraday efficiency of H_2O was as high as 85.0% at 700 °C and 2 V load, while the current efficiency of CO_2 electrolysis was 24.7%. The low value was possibly caused by local CO_2 starvation for the electrochemical reduction under the same conditions used with the H_2O gas. Achieving higher electrolysis performances would require further developments. Effective improvements could be implemented by developing thin-film solid oxide electrolyzers and performing the electrolysis at higher temperatures (Table 1).

References

[1] X. Yang, J.T.S. Irvine, J. Mater. Chem. 18 (2008) 2349.
[2] A. Hauch, S.D. Ebbesen, S.H. Jensen, M. Mogensen, J. Mater. Chem. 18 (2008) 2331.
[3] K. Xie, Y.Q. Zhang, G.Y. Meng, J.T.S. Irvine, J. Mater. Chem. 21 (2011) 195.
[4] S. Dalgaard Ebbesen, M. Mogensen, J. Power Sources 193 (2009) 349.
[5] Z. Zhan, W. Kobsiriphat, J. Wilson, M. Pillai, I. Kim, S.A. Barnett, Energy Fuel 23 (2009) 3089.
[6] K. Xie, Y. Zhang, G. Meng, J.T.S. Irvine, Energy Environ. Sci. 4 (2011) 2118.
[7] S.D. Ebbesen, C. Graves, M. Mogensen, Int. J. Green Energy 6 (2009) 646.
[8] M. Pihlatie, A. Kaiser, M. Mogensen, Solid State Ionics 180 (2009) 1100.
[9] M.H. Pihlatie, H.L. Frandsen, A. Kaiser, M. Mogensen, J. Power Sources 195 (2010) 2677.
[10] S. Tao, J.T.S. Irvine, J. Electrochem. Soc. 151 (2004) A252.
[11] S. Tao, J.T.S. Irvine, J. Kilner, Adv. Mater. 17 (2005) 1734.
[12] D. Bastidas, S. Tao, J.T.S. Irvine, J. Mater. Chem. 16 (2006) 1603.
[13] S. Tao, J.T.S. Irvine, S.M. Plint, J. Phys. Chem. 110 (2006) 21771.
[14] G. Kim, G. Corre, J.T.S. Irvine, J.M. Vohs, R.J. Gorte, Electrochem. Solid-State Lett. 11 (2008) B16.
[15] J.C. Ruiz-Morales, J. Canales-Vazquez, C. Savaniu, D. Marrero-Lopez, W.Z. Zhou, J.T.S. Irvine, Nature 439 (2006) 568.
[16] D. Neagu, J.T.S. Irvine, Chem. Mater. 22 (2010) 5042.
[17] J. Canales-Vazquez, M.J. Smith, J.T.S. Irvine, W.Z. Zhou, Adv. Funct. Mater. 15 (2005) 1000.
[18] K. Xie, R.Q. Yan, X.X. Xu, X.Q. Liu, G.Y. Meng, J. Power Sources 187 (2009) 403.
[19] K. Xie, R.Q. Yan, X.Q. Liu, Electrochem. Commun. 11 (2009) 1618.
[20] M. Ghatee, M.H. Shariat, J.T.S. Irvine, Solid State Ionics 180 (2009) 57.
[21] C. Savaniu, J.T.S. Irvine, J. Mater. Chem. 19 (2009) 8118.
[22] C.O. Park, S.A. Albar, W. Weppenr, J. Mater. Sci. 38 (2003) 4639.
[23] Y. Jiang, A.V. Virkar, J. Electrochem. Soc. 150 (7) (2003) A942.
[24] J. Schefold, A. Brisse, M. Zahid, J. Electrochem. Soc. 156 (2009) B897.